(C(OMe)=OOs) cm^{-1}. Anal. Calcd for $C_{25}H_{49}ClO_5OsP_2$: C, 41.86; H, 6.89. Found: C, 41.60; H, 7.08.

Preparaton of $OsHCl(\eta^2\text{-}O_2)(CO)(PMe\text{-}t\text{-}Bu_2)_2$ (11). Bubbling of O_2 through a suspension of **1** (100.0 mg, 0.18 mmol) in 10 mL of hexane led to solution of the complex and to precipitation of a white solid, which was filtered off, washed with hexane, and dried in vacuo; yield 98 mg (93%). ^1H NMR ($CDCl_3$, 25 °C): δ -3.20 (t, J_{P-H} = 32.0 Hz, 1 H, OsH), 1.50 (vt, N = 14.6 Hz, 18 H, $PCCH_3$), 1.60 (vt, N = 14.6 Hz, 18 H, $PCCH_3$), 1.90 (vt, N = 8.4 Hz, 6 H, PCH_3). ^{31}P NMR ($CDCl_3$, 25 °C): δ 24.87 (s). IR (Nujol): ν(CO) 1955, ν(O-O) 862 cm^{-1}. Anal. Calcd for $C_{19}H_{43}ClO_3OsP_2$: C, 37.59; H, 7.14. Found: C, 37.42; H, 7.53.

Preparation of $OsHCl(\eta^2\text{-}O_2)(CO)(P\text{-}i\text{-}Pr_3)_2$ (12). **12** was prepared by the same procedure as **11** but starting with **2** (100.0 mg, 0.18 mmol): white crystals; yield 98 mg (93%). ^1H NMR ($CDCl_3$, 25 °C): δ -2.40 (t, J_{P-H} = 30.0 Hz, 1 H, OsH), 1.42 (dvt, J_{H-H} = 6.0 Hz, N = 14.0 Hz, 36 H, $PCHCH_3$), 2.90 (m, 6 H, $PCHCH_3$). ^{31}P NMR ($CDCl_3$, 25 °C: δ 25.50 (s). IR (Nujol): ν(Os-H) 2095 (w), ν(CO) 1947 (vs), ν(O-O) 837 cm^{-1}. Anal. Calcd for $C_{19}H_{43}ClO_3OsP_2$: C, 37.59; H, 7.14. Found: C, 37.63; H, 7.62.

Catalytic Reactions. A degassed solution of the catalyst in 2-propanol (4 mL) was syringed through a silicone septum into a 25-mL flask attached to a gas buret, which was in turn connected to a Schlenck manifold. The system was evacuated and refilled with hydrogen three times, and the flask was then inmersed in a constant-temperature bath. The substrate, dissolved in deaerated 2-propanol (4 mL) was subsequently introduced through the septum and the mixture was vigorously shaken during the run. For the experiments involving pretreatment, the catalyst solution was shaken under hydrogen for 30 min at the reaction temperature prior to introduction of the substrate, in one case, or shaken together with the substrate under Ar for 30 min and then evacuated and put under hydrogen. Plots of kinetic data were fitted by use of conventional linear regression programs.

Acknowledgment. We thank the Deutsche Forschungsgemeinschaft, the Fonds der Chemischen Industrie, and the Spanish Ministry of Sciencie and Education, together with DAAD (Acciones Integradas), for generous support of the work. A.A. and R.A.S.-D. thank the University of Zaragoza for Visiting Scientist and Visiting Professor positions, the Spanish Ministry of Science and Education for financial support, and the Venezuelan Institute for Scientific Research (I.V.I.C.) for a sabbatical leave. We also thank U. Neumann and C. P. Kneis for the elemental analysis, Dr. G. Lange, and F. Dadrich for the mass spectra, Dr. M. A. Ciriano for the T_1 measurements, and the Degussa AG (Hanau) for gifts of chemicals.

Registry No. 1, 104911-48-0; **2**, 102513-18-8; **3**, 117526-09-7; **6a**, 122115-86-0; **6b**, 122115-87-1; **6c**, 122115-88-2; **7a**, 104834-23-3; **7b**, 122115-89-3; **7c**, 104834-21-1; **8**, 122115-90-6; **10**, 122115-91-7; **11**, 122115-92-8; **12**, 117526-10-0; CH≡CH, 74-86-2; $CH_3C{\equiv}CH$, 74-99-7; PhC≡CH, 536-74-3; $C_2(CO_2Me)_2$, 762-42-5; styrene, 100-42-5; ethylbenzene, 100-41-4.

Solution and Solid-State Characterization of Europium and Gadolinium Schiff Base Complexes and Assessment of Their Potential as Contrast Agents in Magnetic Resonance Imaging

Paul H. Smith,* James R. Brainard, David E. Morris, Gordon D. Jarvinen, and Robert R. Ryan*

Contribution from the Isotope and Structural Chemistry Division, Group INC-4, MS C346, Los Alamos National Laboratory, Los Alamos, New Mexico 87545.
Received November 17, 1988

Abstract: Two lanthanide Schiff base macrocyclic complexes, $LnHAM(OAc)_2Cl{\cdot}4H_2O$ (Ln = Eu, Gd; HAM = HexaAza-Macrocycle = $C_{22}H_{26}N_6$), have been characterized in view of the potential of the Gd complex as a magnetic resonance imaging (MRI) contrast agent. The relaxivity of $GdHAM(OAc)_2Cl$ was measured at 300 and 20 MHz and is as high as that for the gadolinium aquo ion. The number of coordinated waters, q, was measured by comparison of the luminescent lifetimes of $EuHAM(OAc)_2Cl$ in H_2O and D_2O and found to be between three and four. The complex $GdHAM(OAc)_2Cl{\cdot}4H_2O$ was characterized by single-crystal X-ray diffraction. The complex crystallizes in space group $P\bar{1}$ with Z = 2, a = 10.032 (2) Å, b = 12.765 (2) Å, c = 13.668 (3) Å, α = 69.190° (9)°, β = 72.405° (9)°, and γ = 74.07° (1)°. For 3336 independent data with $I > 3\sigma(I)$, full-matrix least-squares refinement with anisotropic thermal parameters for all non-hydrogen atoms and positional parameters for 8 water hydrogens converged to unweighted and weighted R factors of 3.6% and 4.7%, respectively. The gadolinium ion is 10-coordinate with 6 nitrogen donors from the macrocycle and 4 oxygens from 2 bidentate acetate anions. The four waters and the chloride ion form a hydrogen-bonding network that includes two opposing acetate oxygens. The closest Gd--H distances for the outer-sphere water protons are 4.1 (1) and 4.2 (1) Å. The complexes are stable to decomposition in the presence of oxalate and DTPA in aqueous solution. The reduction potential of $EuHAM(OAc)_2Cl$ in aqueous solution is -0.94 V (versus Ag/AgCl) in 0.1 M KCl, which corresponds to a shift of -270 mV relative to the aquo ion. This indicates a stabilization of Eu(III) relative to Eu(II) in the macrocycle cavity by a factor of $10^{4.6}$.

Paramagnetic compounds are presently undergoing extensive evaluation as contrast agents in magnetic resonance imaging (MRI). These agents increase constrast in MRI by differentially localizing in tissues where they increase the relaxation rates of nearby water protons. Complexes of Gd(III), Fe(III), and Mn(II,III) are under intensive study because their high number of unpaired electrons (S) and long electron-spin relaxation times (T_{1e}) allow efficient relaxation of water protons.[1,2] GdDTPA[3] (DTPA = diethylenetriaminepentaacetic acid) is at present the most commonly used contrast agent because of its large magnetic moment and relatively low toxicity.[2] The high stability constant of GdDTPA reduces toxic effects of Gd(III) by lowering the concentration of free metal ion. However, one factor limiting its effectiveness as a relaxation agent is the availability of only one water coordination site in the complex.[4] The relaxivity[5] of the

(1) Pople, J. A.; Schneider, W. G.; Bernstein, H. J. *High-Resolution Nuclear Magnetic Resonance*; McGraw-Hill: New York, 1959; p 259.
(2) Lauffer, R. B. *Chem. Rev.* **1987**, *87*, 901-927.
(3) GdDTPA is used here to represent a variety of complexes of Gd(III) with DTPA that may be present in aqueous solution, depending on factors such as the pH and concentration of other ligands, e.g., $Gd(DTPA)(H_2O)^{2-}$ or $Gd(HDTPA)(H_2O)^-$.

0002-7863/89/1511-7437$01.50/0

$Gd^{III}DTPA$ complex is a factor of 2–4 lower than that of the Gd^{III} aquo ion.[6] This can be attributed largely to the coordination of eight or nine water molecules in the aquo ion.[2] Therefore, there is significant room for improvement in making contrast agents with higher relaxivities; the challenge is to design metal complexes that have multiple water coordination sites and yet remain intact under physiological conditions.

In addition to the importance of the number of water molecules in the inner coordination sphere (q) and the number of unpaired spins (S), the ligand environment plays an important role in determining the magnitude of the relaxivity of paramagnetic complexes.[7] Geraldes et al.[8] found that the relative relaxivities of two polyaminocarboxylate macrocyclic complexes of Gd(III) were reversed from that predicted based on the number of coordinated waters. In a comparison of the relaxivities of Mn(III) and Fe(III) complexes, Chen et al.[9] showed that $Mn^{III}TPPS$ ($S = 4$) [TPPS = tetrakis(4-sulfophenyl)porphine] has a higher relaxivity than $Fe^{III}TPPS$ ($S = 5$) and $Mn^{II}Cl_2$ ($S = 5$, q for $MnCl_2 > q$ for MnTPPS). Further studies of $Mn^{III}TPPS$ have attributed its high relaxivity to the anisotropy of the ground state wave function of Mn(III), which brings the unpaired spin density of the metal closer to the protons of the coordinated waters than would a spherically symmetric S-state ion.[10] Clearly, the coordination environment can affect the relaxivity of paramagnetic complexes; therefore, the rational design of better MRI contrast agents will require a more detailed understanding of the influence of the structure and dynamics of the ligand on relaxivity and stability.

Tissue differentiation is another desirable property of contrast agents. A strategy with great appeal is to use paramagnetically labeled antibodies which are specific for a particular tissue or pathology.[11] A concern in implementing this strategy is that the concentration of antigenic sites in tissue is estimated to be much less than the concentration at which currently available contrast agents exhibit detectable relaxation effects.[2] Moreover, the rate of antibody accumulation in the antigenic tissue is relatively slow. Thus, the use of GdDTPA conjugated to antibodies poses potential problems of Gd toxicity, since GdDTPA–antibody conjugates have been shown to lose Gd(III) in significant amounts in serum over the length of time (~3 days) required to achieve maximum localization at tumors.[12-14] This emphasizes the need for paramagnetic complexes with enhanced relaxivity and stability.

We considered planar macrocyclic ligands as a means to obtain highly stable complexes of Gd(III), which would also allow coordination of several water molecules for enhanced relaxivity. From this perspective, the reports from the groups of Hart[15] and more recently of Vallarino and Bombieri[16] demonstrating the template synthesis, hydrolytic stability, and water solubility of the lanthanide Schiff base macrocycles illustrated below are especially noteworthy. These complexes provide a potential advantage over GdDTPA in terms of relaxivity enhancement since the ligand denticity is lower, and thus three to four water molecules may coordinate to the metal ion. Furthermore, the ease and versatility of the synthesis of Schiff base macrocycles make them an especially attractive system in which to examine structure–activity relationships. In addition, manganese Schiff base complexes have recently been demonstrated to be effective as imaging agents for liver and kidneys.[17]

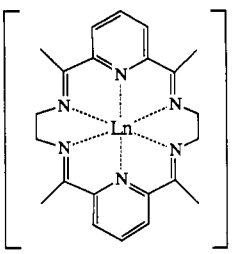

= LnHAM, Ln = La - Lu

We have measured the relaxivity of the gadolinium Schiff base complex and found it to be slightly higher than the Gd^{III}–aquo ion. In an attempt to gain a better understanding of the basis for this high relaxivity, we have investigated the solid-state and solution properties of the europium and gadolinium complexes and report those results here. Ultimately, we hope to develop a rational basis for contrast agent design by identifying the key factors that determine stability and relaxivity.

Table I. Data Collection, Solution, and Refinement Parameters for $GdHAM(OAc)_2Cl{\cdot}4H_2O$

empirical formula	$C_{26}H_{40}N_6O_8Cl_1Gd_1$
formula wt	757.34
crystal system	triclinic
lattice parameters	
a, Å	10.032 (2)
b, Å	12.765 (2)
c, Å	13.668 (3)
α, deg	69.190 (9)
β, deg	72.405 (9)
γ, deg	74.07 (1)
V, Å^3	1532 (1)
space group	$P\bar{1}$ (no. 2)
Z value	2
D_{calc}, g/cm^3	1.64
$F000$	766
μ(Mo Kα), cm^{-1}	23.82
transmission factors (max/min)	1.0/0.79
diffractometer	Enraf-Nonius CAD4
radiation	Mo Kα (λ = 0.71069); graphite monochromated
temp	ambient
$2\text{-}\theta_{max}$, deg	45.0
p factor	0.03
total no. collected	4354
total no. unique	3997
R_{ave} for 277 equiv reflections, %	0.4
av ω scan width at $\theta \cong 12°$, deg	1.02
no. of unique observations ($I > 3\sigma(I)$)	3336
no. of variables	403
residuals: R; R_w	0.036; 0.047
goodness of fit indicator	2.03
largest peak in final diff map, e$^-$/Å^3	1.15; 1.06 Å from Gd

Experimental Section

General. The synthesis of the compounds $LnHAM(OAc)_2Cl{\cdot}4H_2O$ (Ln = Eu, Gd) was accomplished by the method of De Cola et al.,[16] using gadolinium or europium acetate as the template source in the presence of HCl. Elemental analyses were performed by Galbraith Laboratories and were consistent with the formulas $GdC_{26}H_{32}N_6O_4Cl{\cdot}4H_2O$ and $EuC_{26}H_{32}N_6O_4Cl{\cdot}4H_2O$. All starting materials and solvents were reagent grade.

(4) Horrocks, W. D., Jr.; Sudnick, D. R. *J. Am. Chem. Soc.* **1979**, *101*, 334–340.

(5) Relaxivity, R_1, is a measure of the ability of a paramagnetic species to increase the relaxation rate of water protons.

(6) Koenig, S. H.; Brown, R. D., III. *Magnetic Resonance Annual 1987*; Kressel, H. Y., Ed.; Raven: New York, 1987.

(7) Tweedle, M. F.; Gaughan, G. T.; Hagan, J.; Wedeking, P. W.; Sibley, P.; Wilson, L. J.; Lee, D. W. *Nucl. Med. Biol.* **1988**, *15*(1), 31–36.

(8) Geraldes, C. F. G. C.; Sherry, A. D.; Brown, R. D., III; Koenig, S. H. *Magn. Reson. Med.* **1986**, *3*, 242–250.

(9) Chen, C.-W.; Cohen, J. S.; Myers, C. E.; Sohn, M. *FEBS Lett.* **1984**, *168*, 70–74.

(10) Koenig, S. H.; Brown, R. D.; Spiller, M. *Magn. Reson. Med.* **1987**, *4*, 252–260.

(11) Curtet, C.; Bourgoin, C.; Bohy, J.; Saccavini, J.-C.; Thedrez, P.; Akoka, S.; Tellier, C.; Chatal, J.-F. *Int. J. Cancer: Suppl. 2* **1988**, 126–132.

(12) Hnatowich, D. J. *Int. J. Radiat. Appl. Instrum., B* **1986**, *13*, 353–358.

(13) DeNardo, S. J.; DeNardo, G. L.; Peng, J.-S.; Colcher, D. *Radioimmunoimaging and Radioimmunotherapy*; Burchiel, S. V., Rhodes, B. A., Eds.; Elsevier Scientific: New York, 1983; pp 409–417.

(14) Jungerman, J. A.; Yu, K.-H. P.; Zanelli, C. I. *Int. J. Appl. Radiat. Isot.* **1984**, *35*, 883–888.

(15) (a) Backer-Dirks, J. D. J.; Gray, C. J.; Hart, F. A.; Hursthouse, M. B.; Schoop, B. C. *J. Chem. Soc., Chem. Commun.* **1979**, 774–5. (b) Arif, A. M.; Backer-Dirks, J. D. J.; Gray, C. J.; Hart, F. A.; Hursthouse, M. B. *J. Chem. Soc., Dalton Trans.* **1987**, 1665.

(16) (a) De Cola, L.; Smailes, D. L.; Vallarino, L. M. *Inorg. Chem.* **1986**, *25*, 1729–32. (b) Bombieri, G.; Benetollo, F.; Polo, A.; De Cola, L.; Smailes, D. L.; Vallarino, L. M. *Inorg. Chem.* **1986**, *25*, 1127. (c) Bombieri, G. *Inorg. Chim. Acta* **1987**, *139*, 21.

(17) Jackels, S. C.; Kroos, B. R.; Hinson, W. H.; Karstaedt, N.; Moran, P. R. *Radiology* **1986**, *159*(2), 525–30.

Table II. Longitudinal Relaxivities of Selected Gadolinium Complexes

complex	R_1, mM^{-1} s^{-1}	field, T	temp, °C	ref
GdHAM	9.7[a]	7.0	25	this work
$Gd(H_2O)_9$	9.0[a]	7.0	25	this work
GdHAM	9.7[a]	0.47	30	this work
$Gd(H_2O)_9$	9.1	0.47	35	6
GdDTPA	4.1	0.47	35	19
GdEDTA	6.6	0.47	35	19

[a] Correlation coefficients for the relaxivities measured in this work were 0.98–0.99.

Luminescence Measurements. The emission spectra were obtained on a SPEX Fluorolog spectrophotometer equipped with 1200 g/mm holographic gratings. The spectral band-pass was ca. 2.5 nm. Luminescence lifetimes were obtained using the fourth harmonic (266 nm) of a Quanta-Ray DCR-2 Nd:YAG pulsed laser for excitation (ca. 10 mJ/pulse). The emitted light was collected at right angles to the excitation beam and focused in a SPEX Ramalog spectrophotometer equipped with 2400 g/mm gratings. The spectral band-pass was maintained at ca. 5 cm^{-1}. The output of the photomultiplier tube was dropped across a 1-kΩ resistor and monitored with a Hewlett-Packard Model 54111D digital oscilloscope. Between 32 and 64 decay curves were accumulated and averaged by the oscilloscope prior to transfer to an Apple Macintosh II computer. Five to 10 such data sets were summed and fit to a single-exponential decay curve ($R > 0.99$) with Cricket Graph software.

X-ray Crystallography. The data collection and refinement parameters are listed in Table I. Suitable crystals (colorless) were obtained from a benzene/chloroform mixture. Cell constants were determined, and intensity data were collected on a Nonius CAD-4 automated diffractometer using the θ–2θ (variable-speed) scan mode. The space group was confirmed by successful refinement. Data ($h,\pm k,\pm l$) were collected while two intensity standards were monitored every 2 h of X-ray exposure time. The orientation of the same 2 reflections was monitored after every 200th scan. The data were corrected for Lorentz and polarization effects, and an absorption correction was applied with TEXSAN software.[18] No decay or extinction correction was necessary. Absorption was corrected empirically from the average of two ψ scans. The structure was solved with standard Patterson and Fourier methods. Hydrogen atoms for the macrocycle were observed in the difference Fourier map but were placed in idealized positions with isotropic thermal parameters based on their parent carbon atoms (1.2 times) and were not refined. The water hydrogens were also found in the difference Fourier map, and their positional parameters were refined (isotropic thermal parameters calculated as above). Full-matrix least-squares refinements were employed for the reflections with $I > 3\sigma(I)$.

Nuclear Magnetic Resonance and Stability Measurements. Proton relaxation times were measured at 7.0 T at 25 °C and 0.47 T at 30 °C in distilled water, pH 7.4, using inversion recovery pulse sequences, 12–24 τ values, and repetition times of at least $5T_1$. Relaxation times and spectra at 7.0 T were measured on a Bruker WM300, and relaxation times at 0.47 T were measured on a spin-lock spectrometer. The relaxation data at 0.47 T were fit with a least-squares multiexponential fitting program; relaxation data at 7.0 T were least-squares fit to a single exponential using three parameters. All data at both fields exhibited single-exponential behavior. Relaxivities (R_1 in mM^{-1} s^{-1}) were determined from least-squares determinations of the slopes of plots of $1/T_1$ versus concentration of GdHAM, using at least five independent measurements at several concentrations between 0 and 1 mM. Fully relaxed proton spectra of the EuHAM complex were obtained in aqueous solutions and in the presence of DTPA to evaluate the stability of the complex to hydrolysis and to ligand competition. The oxalate was added as the sodium salt, and the solution was stored at room temperature.

Electrochemistry. Data were collected on a PAR Model 303 static mercury drop electrode interfaced to a PAR Model 273 potentiostat, which was in turn interfaced to an IBM PC/AT. The 303 was operated in the HMDE mode (hanging drop) with a large drop size. The EuHAM solution was ca. 2.5 mM and the Eu aquo solution ($EuCl_3 \cdot 6H_2O$) was ca. 2.2 mM. All solutions were made in 0.1 M KCl and were thoroughly purged with nitrogen.

Results and Discussion

Relaxivity. The relaxivities of $GdHAM(OAc)_2Cl$ in aqueous solution (pH 7.4 at 7.0 and 0.47 T) are shown in Table II. These results were obtained from the slope of the plot of $1/T_1$ for the solvent versus complex concentration (Figure 1). The relaxivities for the compounds Gd(III) aquo ion, GdEDTA and GdDTPA are listed for comparison.[6,19] The relaxivity of the GdHAM complex is comparable to that for the Gd^{III} aquo ion, which suggests that the expectation of increased relaxivity in complexes with multiple open coordination sites is realized.

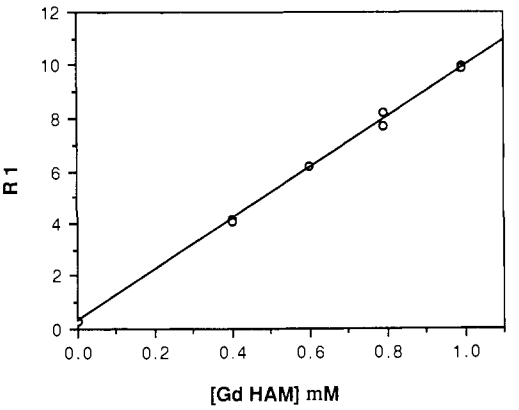

Figure 1. Proton spin–lattice relaxation rates at 7 T, pH 7, and 25 °C as a function of GdHAM concentration (slope = 9.70, r = 0.999).

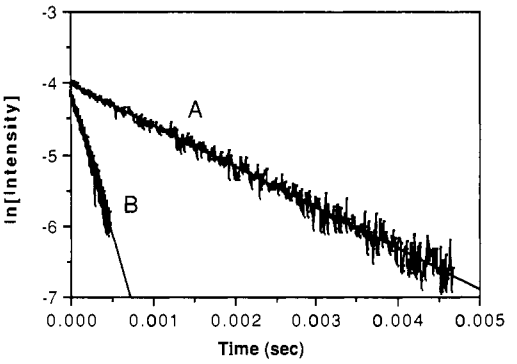

Figure 2. ln plots of luminescence intensity versus time for EuHAM in D_2O (A) and H_2O (B). The solutions were ca. 2 mM. The excitation wavelength was 266 nm, and the detection wavelength was 620 nm.

It is apparent, however, that the relaxivities observed are not solely a function of q. The HAM ligand has a denticity of 6, leaving three to four coordination sites on the metal ion open for water. The Gd^{III} aquo ion has nine coordinated waters and GdDTPA has one.[4] On the basis of the number of coordinated waters, the relaxivity of GdHAM is expected to be between the relaxivities of the aquo ion and GdDTPA. The observation that the relaxivity of GdHAM is as high as that of the aquo ion suggests that q is not the only parameter contributing to the high relaxivity of GdHAM. High relaxivities in similar small chelates of Gd(III) and Mn(III) have been attributed respectively to increases in T_{1e}[8] and to increases in the anisotropy of the unpaired spin distribution.[10] However, it is premature to speculate on the relative contributions of these parameters to the high relaxivity of the GdHAM complex.

Luminescence Lifetime. The number of waters coordinated in an aqueous solution to EuHAM was determined by measuring the luminescence lifetimes in H_2O and D_2O.[20] The deactivation of the $^5D_0$ level of Eu(III) is strongly enhanced by coupling with the OH stretching modes of coordinated water molecules. Thus, the excited-state lifetime of $Eu^{III}_{(aq)}$ is much shorter in H_2O than in D_2O solution. The number of coordinated water molecules is related to the excited-state lifetimes (within an estimated uncertainty of 0.5) by the relationship $q = 1.05\ (k_H - k_D)$, where k_H and k_D are the reciprocals (in ms^{-1}) of the experimental excited-state lifetimes in H_2O and D_2O solutions.[20] The luminescence

(18) TEXSAN, Version 2.0 software, Molecular Structure Corporation, College Station, TX 77840.

(19) Koenig, S. H.; Baglin, C. K.; Brown, R. D., III; Brewer, C. F. *Magn. Reson. Med.* **1984**, *1*, 496.

(20) Horrocks, W. D., Jr.; Albin, M. *Progress in Inorganic Chemistry*; Wiley: New York, 1984; Vol. 31, pp 1–104.

Table III. Positional and Isotropic Thermal Parameters (B_{eq})[a]

atom	x	y	z	B(eq)
Gd	0.19724 (4)	0.30139 (3)	0.26209 (3)	1.81 (3)
Cl	0.1815 (2)	0.9042 (2)	0.1189 (2)	3.7 (2)
O1	0.2700 (6)	0.4621 (5)	0.2768 (4)	3.2 (5)
O2	0.3111 (6)	0.4523 (4)	0.1134 (4)	3.0 (5)
O3	0.0029 (6)	0.1949 (5)	0.3325 (5)	3.5 (5)
O4	0.2151 (6)	0.0902 (5)	0.3324 (4)	3.1 (5)
O5	0.3741 (8)	0.8871 (7)	0.2785 (6)	4.7 (7)
O6	0.152 (1)	-0.014 (1)	0.8745 (5)	5.3 (7)
O7	0.448 (1)	0.4383 (8)	0.4166 (8)	6.4 (9)
O8	0.478 (1)	0.3474 (7)	0.6355 (8)	7 (1)
N1	0.0981 (6)	0.3103 (5)	0.1015 (5)	2.1 (5)
N2	0.3643 (6)	0.2068 (5)	0.1132 (5)	2.3 (5)
N3	0.4578 (6)	0.2263 (5)	0.2757 (5)	2.4 (5)
N4	0.2581 (7)	0.2355 (5)	0.4525 (5)	2.1 (5)
N5	0.0097 (7)	0.3660 (6)	0.4239 (5)	2.9 (6)
N6	-0.0279 (7)	0.4516 (5)	0.2177 (5)	2.4 (5)
C1	0.1676 (8)	0.2427 (6)	0.0385 (6)	2.1 (6)
C2	0.3194 (8)	0.1967 (6)	0.0394 (6)	2.4 (6)
C3	0.407 (1)	0.1441 (8)	-0.0473 (7)	4.0 (8)
C4	0.5115 (9)	0.1615 (7)	0.1195 (6)	3.0 (7)
C5	0.5583 (8)	0.2284 (7)	0.1721 (7)	2.9 (7)
C6	0.5033 (8)	0.1907 (6)	0.3614 (6)	2.4 (6)
C7	0.655 (1)	0.1568 (9)	0.3709 (8)	4.5 (9)
C8	0.3907 (8)	0.1854 (6)	0.4633 (6)	2.4 (6)
C9	0.423 (1)	0.1326 (7)	0.5637 (7)	3.4 (7)
C10	0.315 (1)	0.1331 (8)	0.6531 (7)	4.0 (8)
C11	0.179 (1)	0.1872 (7)	0.6422 (6)	3.5 (8)
C12	0.1533 (9)	0.2393 (6)	0.5410 (6)	2.4 (6)
C13	0.0124 (9)	0.3105 (7)	0.5216 (6)	2.6 (7)
C14	-0.112 (1)	0.3159 (8)	0.6142 (7)	3.9 (8)
C15	-0.1208 (9)	0.4462 (8)	0.4025 (7)	3.7 (8)
C16	-0.0872 (9)	0.5240 (7)	0.2895 (7)	3.1 (7)
C17	-0.1046 (8)	0.4409 (6)	0.1646 (6)	2.4 (6)
C18	-0.257 (1)	0.4976 (8)	0.1639 (8)	3.9 (8)
C19	-0.0373 (8)	0.3634 (6)	0.0975 (6)	2.2 (6)
C20	-0.1069 (8)	0.3455 (7)	0.0332 (7)	3.0 (7)
C21	-0.037 (1)	0.2711 (7)	-0.0270 (7)	3.5 (8)
C22	0.102 (1)	0.2209 (7)	-0.0257 (6)	3.0 (7)
C23	0.3201 (8)	0.4997 (6)	0.1767 (7)	2.7 (7)
C24	0.390 (1)	0.6012 (7)	0.1329 (7)	3.6 (8)
C25	0.084 (1)	0.0991 (7)	0.3453 (6)	2.5 (7)
C26	0.023 (1)	-0.0051 (8)	0.3719 (7)	3.7 (8)
H33	0.32 (1)	0.957 (8)	0.311 (8)	5.7
H34	0.33 (1)	0.88 (1)	0.25 (1)	5.7
H35	0.06 (1)	0.01 (1)	0.858 (9)	6.5
H36	0.16 (2)	-0.03 (1)	0.91 (1)	6.5
H37	0.46 (1)	0.52 (1)	0.41 (1)	7.7
H38	0.39 (2)	0.45 (1)	0.40 (1)	7.7
H39	0.55 (1)	0.31 (1)	0.61 (1)	8.1
H40	0.47 (1)	0.38 (1)	0.56 (1)	8.1

[a] Estimated standard deviations in the least significant figure are given in parentheses in this and subsequent tables.

decay curves are plotted for D_2O (A) and H_2O (B) in Figure 2. The rate constants for the luminescence decay of EuHAM in H_2O and D_2O are 3.92 ± 0.07 and 0.57 ± 0.02, respectively. This indicates that the value of q is between 3 and 4 and implies a 9–10-coordinate metal ion in dilute aqueous solution. Sabbatini and co-workers have measured the value of q for EuHAM in 0.1 M sodium acetate by this method.[21] They report a value of q = 1, indicating that one acetate ion is coordinated under these conditions.

Crystal Structure. The single-crystal X-ray structure of $[GdHAM(OAc)_2]Cl\cdot 4H_2O$ has been determined in order to provide an estimate for the number of potential coordination sites for water. The labeling diagram and stereoviews of the $[GdHAM(OAc)_2]$ cation are illustrated in Figures 3 and 4, respectively. The positional parameters are listed in Table III. Bond distances and angles are listed in Tables IV and V, respectively. The gadolinium ion is 10-coordinate with 6 nitrogens from the macrocycle and 4 oxygens from 2 bidentate acetate anions bound

(21) Sabbatini, N.; De Cola, L.; Vallarino, L. M.; Blasse, G. *J. Phys. Chem.* **1987**, *91*, 4681.

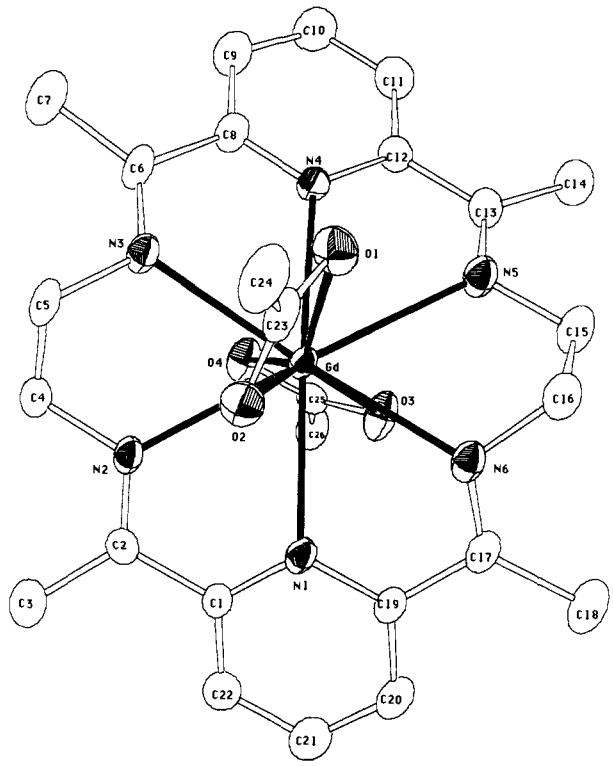

Figure 3. ORTEP labeling diagram for $[GdHAM(OAc)_2]^+$.

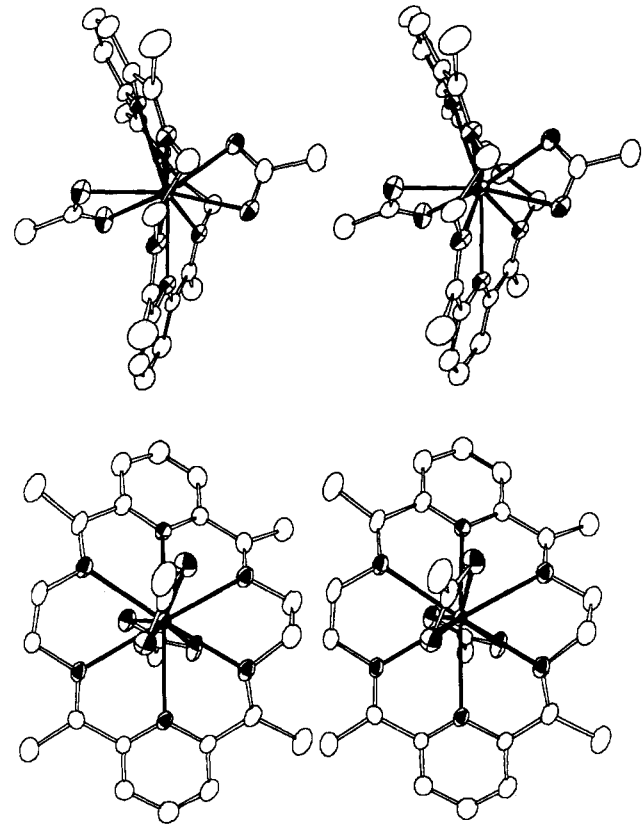

Figure 4. ORTEP stereoviews of $[GdHAM(OAc)_2]^+$ showing top view (bottom) and side view (top).

to the metal. The Gd atom lies 0.05 Å from the least-squares plane defined by the six nitrogens, and the mean deviation of the nitrogens from that plane is 0.36 Å. The acetate ions are coordinated on opposite sides of the metal ion, and the dihedral angle between the planes of the two Gd(OAc) fragments is 95.1°. The fact that the complex is 10-coordinate suggests that in aqueous solution the number of available coordination sites for water would

Table IV. Intramolecular Bond Distances[a]

atom	atom	distance	atom	atom	distance
Gd	O3	2.442 (5)	C1	C2	1.48 (1)
Gd	O1	2.446 (5)	C2	C3	1.50 (1)
Gd	O2	2.484 (5)	C4	C5	1.53 (1)
Gd	O4	2.494 (5)	C6	C7	1.49 (1)
Gd	N3	2.565 (6)	C6	C8	1.50 (1)
Gd	N6	2.602 (6)	C8	C9	1.39 (1)
Gd	N1	2.627 (6)	C9	C10	1.37 (1)
Gd	N4	2.642 (6)	C10	C11	1.37 (1)
Gd	N2	2.643 (6)	C11	C12	1.38 (1)
Gd	N5	2.654 (6)	C12	C13	1.50 (1)
O1	C23	1.27 (1)	C13	C14	1.49 (1)
O2	C23	1.25 (1)	C15	C16	1.50 (1)
O3	C25	1.25 (1)	C17	C19	1.48 (1)
O4	C25	1.25 (1)	C17	C18	1.50 (1)
N1	C1	1.35 (1)	C19	C20	1.38 (1)
N1	C19	1.35 (1)	C20	C21	1.38 (1)
N2	C2	1.28 (1)	C21	C22	1.37 (1)
N2	C4	1.45 (1)	C23	C24	1.49 (1)
N3	C6	1.27 (1)	C25	C26	1.50 (1)
N3	C5	1.47 (1)	O5	H34	0.7 (1)
N4	C8	1.34 (1)	O5	H33	1.1 (1)
N4	C12	1.35 (1)	O6	H36	0.5 (1)
N5	C13	1.27 (1)	O6	H35	1.0 (1)
N5	C15	1.46 (1)	O7	H38	0.6 (1)
N6	C17	1.27 (1)	O7	H37	1.1 (1)
N6	C16	1.47 (1)	O8	H39	0.8 (1)
C1	C22	1.38 (1)	O8	H40	1.0 (1)

[a] Distances are in angstroms.

be between 3 and 4, which is indeed what is observed for EuHAM from the luminescent lifetime measurements.

A number of structures of lanthanide HAM complexes have been determined, and a common feature of these structures is that the two diiminopyridine fragments are not coplanar.[15,16] The dihedral angle between the two planes has been used as a measure of this noncoplanarity, and it ranges from 27° for La to 69° for Eu, indicating that the macrocycle is quite flexible at the ethylenediamine "hinges". The dihedral angle for the GdHAM complex reported here is 48°. This dihedral angle has two components: a "bending" at the ethylenediamine hinges and a "twisting" about an axis through the pyridine nitrogens. The conformation of the macrocycles across the lanthanide series ranges from being almost purely twisted for the La complex to primarily bent for the Lu complex. The Gd macrocycle appears to be some combination of these two extremes. These distortions would be expected to decrease the cavity size of the macrocycle relative to a planar form. However, there appears to be no simple correlation between the degree of bend/twist character and the ionic radii of the metal, since the Ce and Nd complexes appear to be more like the Lu complex than the La complex.[15,16]

A comparison of the Gd–N bond lengths in the HAM complexes to those in similar acyclic Schiff base complexes provides additional information about the cavity size of the macrocycle relative to the metal ion size. One ligand for comparison is the condensation product of two 2-formylpyridines with ethylenediamine.[22] The Gd ion is coordinated by four nitrogens from the Schiff base ligand and six oxygens from three bidentate nitrate anions. Because both this complex and the GdHAM complex are 10-coordinate, the bond lengths can be compared directly. The average Gd–N bond length in the acyclic analogue is 2.54 Å, as compared to 2.62 Å in the macrocyclic case. A similar comparison can be made to a 10-coordinate cerium(III) complex, bis[2,6-diacetylpyridine bis(semicarbazone)]cerium(III) perchlorate.[23] The average of the six Ce–N bonds is 2.68 Å. Assuming a 0.09-Å decrease[24] in bond lengths from Ce(III) to Gd(III), the Gd complex would be expected to have an average Gd–N distance of 2.59 Å. Again, the Gd–N bond lengths are longer in the macrocyclic complex than those predicted for the acyclic analogue. If it is assumed that the M–N distances in the acyclic cases represent "nonconstrained" Gd–N bond lengths, then the rather long distances in the macrocyclic complex can be attributed to a slight cavity size/metal size mismatch.

Finally, a hydrogen-bonding network, which includes the four water molecules (O5–O8 and H33–H40) and the chloride ion, extends from two opposing acetate oxygens (O1 and O4) and forms an infinite chain that interconnects the Gd complexes. The oxygen–oxygen contacts range from 2.82 (1) to 2.95 (1) Å, and the oxygen–chloride contacts range from 3.206 (7) to 3.243 (7) Å. The closest approach of outer-sphere water hydrogens to the Gd atom is illustrated by the protons that are hydrogen-bonded to the acetate oxygens. These distances are 4.2 (1) Å (Gd–H38) and 4.1 (1) Å (Gd–H33). A similar Gd–H distance for outer-sphere water protons would be expected when the acetates are

Table V. Intramolecular Bond Angles[a]

atom	atom	atom	angle	atom	atom	atom	angle
O3	Gd	O1	141.7 (2)	C19	N1	Gd	118.8 (5)
O3	Gd	O2	147.0 (2)	C2	N2	C4	119.7 (6)
O3	Gd	O4	52.4 (2)	C2	N2	Gd	122.9 (5)
O3	Gd	N3	127.8 (2)	C4	N2	Gd	117.4 (5)
O3	Gd	N6	74.7 (2)	C6	N3	C5	120.0 (7)
O3	Gd	N1	71.0 (2)	C6	N3	Gd	126.1 (5)
O3	Gd	N4	92.0 (2)	C5	N3	Gd	113.9 (5)
O3	Gd	N2	101.7 (2)	C8	N4	C12	119.3 (6)
O3	Gd	N5	69.2 (2)	C8	N4	Gd	119.9 (5)
O1	Gd	O2	52.7 (2)	C12	N4	Gd	120.3 (5)
O1	Gd	O4	143.7 (2)	C13	N5	C15	117.6 (7)
O1	Gd	N3	75.9 (2)	C13	N5	Gd	121.8 (5)
O1	Gd	N6	83.7 (2)	C15	N5	Gd	118.4 (5)
O1	Gd	N1	124.1 (2)	C17	N6	C16	120.2 (7)
O1	Gd	N4	73.2 (2)	C17	N6	Gd	122.4 (5)
O1	Gd	N2	116.4 (2)	C16	N6	Gd	113.8 (5)
O1	Gd	N5	72.9 (2)	N1	C1	C22	121.8 (7)
O2	Gd	O4	141.8 (2)	N1	C1	C2	115.9 (6)
O2	Gd	N3	79.9 (2)	C22	C1	C2	122.2 (7)
O2	Gd	N6	79.9 (2)	N2	C2	C1	117.1 (6)
O2	Gd	N1	78.3 (2)	N2	C2	C3	126.1 (7)
O2	Gd	N4	119.6 (2)	C1	C2	C3	116.8 (7)
O2	Gd	N2	72.5 (2)	N2	C4	C5	109.7 (6)
O2	Gd	N5	116.6 (2)	N3	C5	C4	107.9 (6)
O4	Gd	N3	76.3 (2)	N3	C6	C7	127.4 (7)
O4	Gd	N6	126.3 (2)	N3	C6	C8	115.5 (7)
O4	Gd	N1	91.1 (2)	C7	C6	C8	117.2 (7)
O4	Gd	N4	73.0 (2)	N4	C8	C9	121.7 (7)
O4	Gd	N2	70.4 (2)	N4	C8	C6	116.4 (6)
O4	Gd	N5	101.0 (2)	C9	C8	C6	121.9 (7)
N3	Gd	N6	157.3 (2)	C10	C9	C8	118.6 (8)
N3	Gd	N1	124.4 (2)	C9	C10	C11	119.8 (8)
N3	Gd	N4	61.1 (2)	C10	C11	C12	119.4 (8)
N3	Gd	N2	64.2 (2)	N4	C12	C11	121.1 (8)
N3	Gd	N5	118.7 (2)	N4	C12	C13	115.9 (6)
N6	Gd	N1	60.5 (2)	C11	C12	C13	122.8 (7)
N6	Gd	N4	122.2 (2)	N5	C13	C14	124.3 (8)
N6	Gd	N2	118.5 (2)	N5	C13	C12	115.8 (7)
N6	Gd	N5	62.9 (2)	C14	C13	C12	119.9 (7)
N1	Gd	N4	161.9 (2)	N5	C15	C16	108.1 (7)
N1	Gd	N2	60.6 (2)	N6	C16	C15	107.3 (6)
N1	Gd	N5	116.8 (2)	N6	C17	C19	116.4 (7)
N4	Gd	N2	119.3 (2)	N6	C17	C18	126.8 (7)
N4	Gd	N5	59.9 (2)	C19	C17	C18	116.8 (7)
N2	Gd	N5	170.5 (2)	N1	C19	C20	121.0 (7)
C25	Gd	C23	178.1 (3)	N1	C19	C17	116.2 (6)
C23	O1	Gd	94.1 (5)	C20	C19	C17	122.8 (7)
C23	O2	Gd	92.7 (5)	C21	C20	C19	119.5 (8)
C25	O3	Gd	94.3 (5)	C22	C21	C20	119.0 (7)
C25	O4	Gd	91.9 (5)	C21	C22	C1	119.4 (7)
H34	O5	H33	104 (1)	O2	C23	O1	120.5 (7)
H36	O6	H35	122 (2)	O2	C23	C24	119.3 (8)
H38	O7	H37	98 (2)	O1	C23	C24	120.2 (8)
H39	O8	H40	83 (1)	O4	C25	O3	120.8 (7)
C1	N1	C19	119.1 (6)	O4	C25	C26	119.7 (8)
C1	N1	Gd	120.4 (5)	O3	C25	C26	119.4 (8)

[a] Angles are in degrees.

(22) Smith, G. D.; Caughlan, C. N.; Mazhar-Ur-Haque; Hart, F. A. *Inorg. Chem.* **1973**, *12*, 2654–2658.
(23) Thomas, J. E.; Palenik, G. J. *Inorg. Chim. Acta* **1980**, *44*, L303–L304.
(24) Shannon, R. D. *Acta. Crystallogr.* **1976**, *A32*, 751–767. Changes in bond lengths due to the lanthanide contraction were estimated from the differences in ionic radii for 9-coordinate complexes.

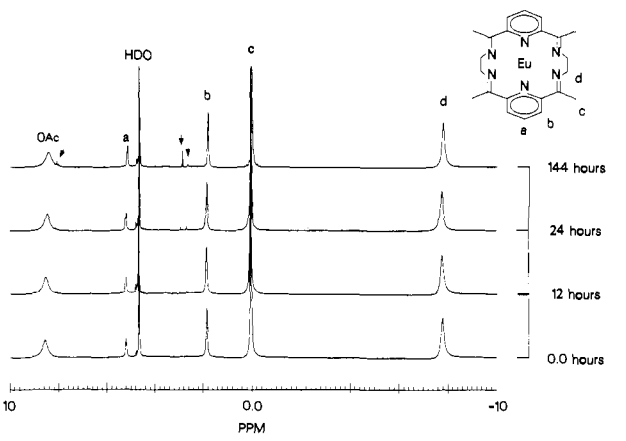

Figure 5. ^{1}H NMR spectra of the EuHAM complex at 25 °C and pH 6.6. The assignments are indicated in the figure: 8.43 ppm OAc, 5.17 ppm (triplet) a_{pyr}, 2.78 ppm (doublet) b_{pyr}, 0.04 ppm CH_3, 7.78 ppm CH_2. The small resonances from decomposition of the EuHAM complex are indicated by the arrows.

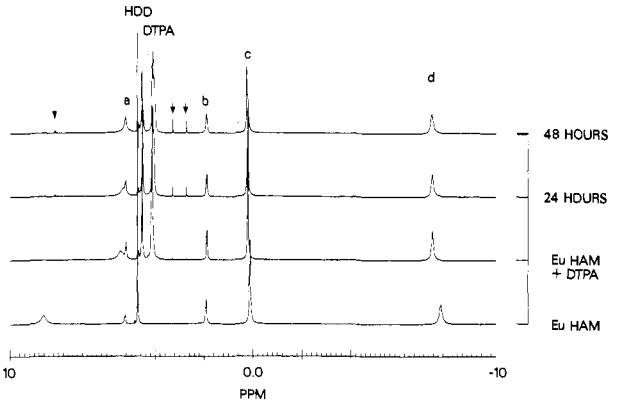

Figure 6. ^{1}H NMR spectra of the EuHAM complex at 25 °C, pH 6.2, in the presence of a 2-fold excess of DTPA. The added DTPA competes with acetate for coordination sites on the complex, causing a ~3 ppm upfield shift of the acetate proton resonance and small shifts of the HAM macrocycle resonances. The small resonances from decomposition of the EuHAM complex are indicated by the arrows.

replaced by coordinated water molecules in aqueous solution. This distance may be used to estimate the relative contributions of outer-sphere (H-bonded) versus inner-sphere water protons to the relaxivity. Assuming a $1/r^6$ dependence of the relaxivity on the metal–proton distance and using 3.13 Å as a typical Gd–H distance for a coordinated water proton,[2] the contribution to the relaxivity from an outer-sphere H-bonded proton is expected to be approximately one-fifth of that from a coordinated water proton. Thus, a significant portion of the relaxivity may arise from this hydrogen-bonding mechanism.

Solution Structure and Stability. The flexibility of the macrocycle is supported experimentally by the degeneracies in the ^{1}H and ^{13}C NMR spectra in solution. Assignments were made based on multiplicities, integrated intensities, and addition of acetate to solutions of the complex and are indicated in Figure 5. The symmetry of the complex at room temperature in aqueous solution is D_{2h}, and therefore the bending of the two diiminopyridine portions of the macrocycle about the diamine bridges is rapid on the NMR time scale.

The hydrolytic stability of the EuHAM complexes was evaluated by ^{1}H and ^{13}C NMR spectra in neutral and acidic aqueous solutions. Proton spectra of $EuHAM(OAc)_2Cl$ at pH 6.6 are shown in Figure 5. The proton spectra show minor changes over a 6-day period; small resonances appear at 2.67, 2.89, and 8.09 ppm. The combined integrated intensity of these new resonances after 6 days is 2.2% of the total proton intensity of the complex. The rate of appearance of very similar resonances (2.74, 3.29, and 8.15 ppm) is slightly increased by the addition of a 2-fold excess of DPTA as shown in Figure 6 (3.9% of total intensity after 48 h). The ^{13}C spectra of the complex show no evidence for decomposition at pH 2.5 after 14 h.

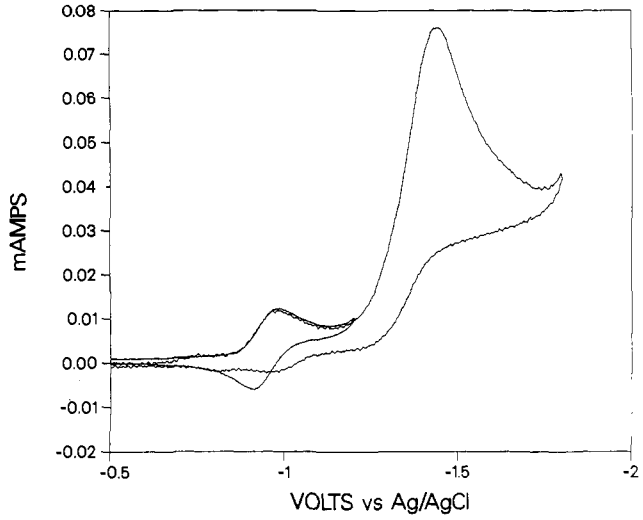

Figure 7. Cyclic voltammograms of EuHAM in 0.1 M KCl at 0.1 V/s illustrating the loss of reversibility upon scanning to more negative potentials.

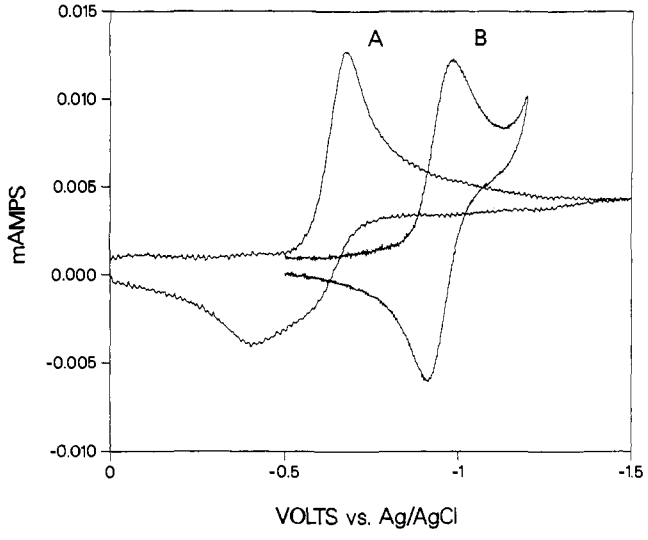

Figure 8. Comparison of complexed and uncomplexed Eu(III)/Eu(II) cyclic voltammograms in 0.1 M KCl at 0.1 V/s. Curve A is the Eu aquo ion and curve B is the EuHAM complex.

The stability of the GdHAM complex against decomposition in the presence of the precipitating agent, oxalate, has also been evaluated. Under conditions of excess oxalate (pH 9.4, total [Ox] = 0.067 M, total [GdHAM] = 0.006 M), no precipitate was observed over a 24-h period. After that period, a precipitate accumulated slowly over a period of several days. Assuming that the precipitate is Gd_2Ox_3, this observation implies that the complex stability is due to a kinetic rather than a thermodynamic phenomenon.

Electrochemistry. The cyclic voltammetry of the EuHAM complex in aqueous solution shows the two reduction waves illustrated in Figure 7. The first wave at −0.94 V versus Ag/AgCl is reversible and has been assigned to the Eu(III)/Eu(II) couple.[25] The second wave is irreversible and is presumed to be a ligand-based reduction. An expansion of the Eu(III)/Eu(II) portion is illustrated in Figure 8B. This can be compared to the reduction

(25) This assignment is based on a comparison of the cyclic voltammogram to that of the corresponding TbHAM complex, which shows only the more negative reduction wave. The cyclic voltammograms for the EuHAM complex showed no scan rate dependence over the range 0.01–1.0 V/s, indicating that the couple is electrochemically reversible.

of the Eu^{III} aquo ion ($EuCl_3$) illustrated in Figure 8A, which is quasi-reversible. The reversible behavior gained upon complexation by the macrocycle is also observed in the Eu[2.2.1]- and Eu[2.2.2]cryptates and in similar Eu macrocyclic amine complexes.[26,27] The reduction potential of EuHAM is shifted approximately -270 mV relative to the potential for the aquo ion. This potential shift can be used to calculate the relative complex stability in the two oxidation states.[26] The measured shift corresponds to a stabilization by a factor of $10^{4.6}$ of Eu(III) relative to Eu(II) in the macrocycle. This contrasts with the positive shifts of 200 and 420 mV observed for the Eu[2.2.1]- and Eu[2.2.2]-cryptate complexes, respectively. These positive shifts were attributed largely to a better fit of Eu(II) in the cryptate cavities.[26] This suggests that the cavity size of the HAM ligand is much better suited to the +3 state than the +2 state. The ionic radius of Eu(II) is slightly larger (0.08 Å for 10-coordinate complexes) than that of La(III).[24]

Conclusion. The GdHAM complex shows significant promise as an MRI contrast agent because of its high relaxivity and kinetic stability. Both the GdHAM crystal structure and the EuHAM luminescent lifetime measurements indicate three to four open coordination sites for water. The hydrogen bonds to two coordinated acetate oxygens in the solid state provide an estimate for the closest approach of an outer-sphere water proton of 4.1-4.2 Å. The cavity size of the macrocycle appears to be slightly too large for Gd(III) based on a comparison of Ln-N bond lengths to acyclic analogues. This observation, in conjunction with the Eu(III)/Eu(II) redox potential, suggests that the optimum metal ion size for the HAM cavity is somewhere between the radii of Gd(III) and Eu(II). While the structural and dynamic properties responsible for the high relaxivity and stability of this complex need to be more completely defined, the concept of designing planar macrocyclic ligands for Gd(III) clearly shows potential for producing improved MRI contrast agents.

Acknowledgment. We are grateful to Dr. D. Smith for the use of the spin-lock NMR spectrometer, Drs. P. M. Killough and C. D. Tait for assistance with the luminescence lifetime measurements, Dr. C. J. Burns for help with the X-ray crystallography, and Dr. J. H. Hall for assistance with molecular modeling calculations. We appreciate helpful discussions with Dr. C. B. Storm, our colleagues at the Center for Non-Invasive Diagnosis, and the Medical Radioisotopes group at LANL. P.H.S. would like to acknowledge postdoctoral funding from the Director of the Laboratory.

Registry No. $[GdHAM(OAc)_2]Cl\cdot 4H_2O$, 122114-27-6; $[EuHAM(OAc)_2]Cl\cdot 4H_2O$, 122093-05-4.

Supplementary Material Available: Figure S1 showing the emission spectrum of EuHAM in aqueous solution, Table S2 listing the anisotropic thermal parameters for non-hydrogen atoms, and Table S3 listing the calculated positional and thermal parameters for hydrogen atoms (3 pages); Table S1 listing calculated and observed structure factors (23 pages). Ordering information is given on any current masthead page.

(26) Yee, E. L.; Gansow, O. A.; Weaver, M. J. *J. Am. Chem. Soc.* **1980**, *102*, 2278-2285.
(27) Smith, P. H.; Reyes, Z. E.; Lee, C.-W.; Raymond, K. N. *Inorg. Chem.* **1988**, *27*, 4154.

Alkene Epoxidations Catalyzed by Iron(III), Manganese(III), and Chromium(III) Porphyrins. Effects of Metal and Porphyrin Substituents on Selectivity and Regiochemistry of Epoxidation

Teddy G. Traylor* and Andrew R. Miksztal

Contribution from the Department of Chemistry, D-006, University of California, San Diego, La Jolla, California 92093. *Received February 3, 1989*

Abstract: The products of epoxidation of norbornene, cyclohexene, and adamantylideneadamantane with pentafluoroiodobenzene using as catalysts variously substituted tetraphenylporphyrin complexes of chloroiron(III), chloromanganese(III), and chlorochromium(III) have been determined. All catalysts afforded the epoxide from adamantylideneadamantane, suggesting that the metallacycle intermediate, impossible in this case, is not required for epoxidation. The ratios of *exo*- to *endo*-epoxynorbornanes obtained from norbornene varied from about 10^3 for electropositively substituted Cr(III) complexes gradually through the Mn(III) and Fe(III) series to a value of about 6 for electronegatively substituted iron(III) porphyrins. Mechanisms ranging from limiting electrophilic addition to limiting electron transfer are proposed to account for these changes. The electronegatively substituted iron porphyrins show a greater tendency toward epoxidation rather than allylic oxidation and show more selectivity for *cis*-alkenes.

The epoxidation of alkenes remains an important synthetic process. Recent development of metal-catalyzed epoxidations has encouraged further attempts to develop more selective and more commercially attractive epoxidation reactions.[1]

Among the transition-metal catalysts for oxygen transfer the metalloporphyrins offer some attractive advantages.[2-9] They provide a strong four-coordinate ligand, which can be very stable toward destruction and has a potential for elaboration to provide

(1) (a) Sheldon, R. A.; Kochi, J. K. *Metal Catalyzed Oxidations of Organic Compounds*; Academic Press: New York, 1981. (b) Srinavasan, K. Michaud, P.; Kochi, J. K. *J. Am. Chem. Soc.* **1986**, *108*, 2309. (c) Samuelson, E. G.; Srinavasan, K.; Kochi, J. K. *J. Am. Chem. Soc.* **1985**, *107*, 7606.
(2) (a) Groves, J. T.; Nemo, T. E.; Myers, R. S. *J. Am. Chem. Soc.* **1979**, *101*, 1032. (b) Groves, J. T.; Kruper, W. J., Jr.; Haushalter, R. C. *Ibid.* **1980**, *102*, 6375. (c) Groves, J. T.; Kruper, W. J.; Nemo, T. E.; Myers, R. S. *J. Mol. Catal.* **1980**, *7*, 169.
(3) (a) Mansuy, D.; Bartoli, J.-F.; Momenteau, M. *Tetrahedron Lett.* **1982**, *23*, 2781. (b) Mansuy, D. *Pure Appl. Chem.* **1987**, *59*, 759, and references cited there.
(4) Guilmet, E.; Meunier, B. *Tetrahedron Lett.* **1980**, *21*, 4449.
(5) Suslick, K. S.; Cook, B. R. *J. Chem. Soc., Chem. Commun.* **1987**, 200.
(6) Lindsay-Smith, J. R.; Sleath, P. R. *J. Chem. Soc., Perkin Trans. 2* **1982**, 1009.
(7) Traylor, T. G.; Nakano, T.; Dunlap, B. E.; Traylor, P. S.; Dolphin, D. *J. Am. Chem. Soc.* **1986**, *108*, 2782.
(8) (a) Collman, J. P.; Kodadek, T.; Raybuck, S. A.; Brauman, J. I.; Papazian, L. M. *J. Am. Chem. Soc.* **1985**, *107*, 4343. (b) Razenberg, J. A. S. J.; Nolte, R. J. M.; Drenth, W. *J. Chem. Soc., Chem. Commun.* **1986**, 277.

0002-7863/89/1511-7443$01.50/0